(2)

OFFICE OF NAVAL RESEARCH

Contract N00014-91-J-1927

R&T Code 413v001

Technical Report No. 7

SIMULATIONS OF SOLVENT EFFECTS ON CONFINED ELECTROLYTES

by

LIANRUI ZHANG, H. TED DAVIS, AND HENRY S. WHITE

Prepared for Publication in

JOURNAL OF CHEMICAL PHYSICS

University of Minnesota
Department of Chemical Engineering and Materials Science
Minneapolis, MN 55455

March 20, 1993

REPORT DOCUMENTATION PAGE

Form Approved
OMB No. 0704-0188

1. AGENCY USE ONLY (Leave blank)	2. REPORT DATE	3. REPORT TYPE AND DATES COVERED
	March 20, 1993	Technical 6/30/92 - 3/31/93

4. TITLE AND SUBTITLE

SIMULATIONS OF SOLVENT EFFECTS ON CONFINED ELECTROLYTES

5. FUNDING NUMBERS

N00014-91-J-1927

6. AUTHOR(S)

LIANRUI ZHANG, H. TED DAVIS, AND HENRY S. WHITE

7. PERFORMING ORGANIZATION NAME(S) AND ADDRESS(ES)

Dept. of Chemical Engineering and Materials Science
University of Minnesota

8. PERFORMING ORGANIZATION REPORT NUMBER

Technical Report No. 7

9. SPONSORING/MONITORING AGENCY NAME(S) AND ADDRESS(ES)

Office of Naval Research
800 North Quincy Street
Arlington, VA 22217

10. SPONSORING/MONITORING AGENCY REPORT NUMBER

11. SUPPLEMENTARY NOTES

12a. DISTRIBUTION/AVAILABILITY STATEMENT

Unclassified/Unlimited

12b. DISTRIBUTION CODE

13. ABSTRACT (Maximum 200 words)

Monte Carlo simulations are reported for the solvent primitive model (SPM) of the electrical double layer at electrically charged and neutral surfaces. Both solvent and ions are modeled as hard spheres with interactions governed by hard sphere and Coulomb interactions. Density profiles of solvent and ions and electrostatic potential profiles are presented for 1:1 electrolyte concentrations of 1 and 2M at 300K. Comparison of results at charged and neutral walls indicates that the density distribution of a dense solvent near a wall induces significant layering of ions and decrease of potentials in the double layer. This layering effect cannot be captured in simulations of the conventional primitive model (PM) of the double layer. The solvent induced steric ordering of electrolyte ions at a neutral wall can create a space charge layer.

14. SUBJECT TERMS			15. NUMBER OF PAGES 20
			16. PRICE CODE
17. SECURITY CLASSIFICATION OF REPORT	18. SECURITY CLASSIFICATION OF THIS PAGE	19. SECURITY CLASSIFICATION OF ABSTRACT	20. LIMITATION OF ABSTRACT
Unclassified	UL		

NSN 7540-01-280-5500

Standard Form 298 (Rev. 2-89)
Prescribed by ANSI Std. Z39-18
298-102

SIMULATIONS OF SOLVENT EFFECTS ON CONFINED ELECTROLYTES

Lianrui Zhang, H. Ted Davis, Henry S. White

Department of Chemical Engineering and Materials Science
University of Minnesota
Minneapolis, MN 55455

Abstract

Monte Carlo simulations are reported for the solvent primitive model (SPM) of the electrical double layer at electrically charged and neutral surfaces. Both solvent and ions are modeled as hard spheres with interactions governed by hard sphere and Coulomb interactions. Density profiles of solvent and ions and electrostatic potential profiles are presented for 1:1 electrolyte concentrations of 1 and 2M at 300K. Comparison of results at charged and neutral walls indicates that the density distribution of a dense solvent near a wall induces significant layering of ions and decrease of potentials in the double layer. This layering effect cannot be captured in simulations of the conventional primitive model (PM) of the double layer. The solvent induced steric ordering of electrolyte ions at a neutral wall can create a space charge layer.

J. Chem. Phys.

I. Introduction

Separation of charge in the vicinity of a surface that is either charged or neutral occurs in a variety of phenomena in electrochemical, biological, tribological, and colloidal sciences. For low surface charge and dilute electrolyte solutions, the classical theory of Gouy [1] and Chapman [2], and later modified by Stern (GCS) [3] gives predictions of the interfacial ion and potential distributions that are in excellent agreement with experiment and computer simulations. More recent theoretical and computational studies have demonstrated that the detailed structure of the solvent and ion are fundamental to accurately describe the interfacial double layer properties for highly coupled systems at high bulk ion densities. Among the models of the electrical double layer, the most widely used is the primitive model (PM), in which ions are represented as point charges that are embedded in hard spheres, the solvent is modeled as an isotropic dielectric continuum, and the surface modeled as a hard wall with uniform surface charge density. Vigorous investigation of the PM by computer simulations [4-11], integral equation methods, and functional theories [12-19] during the last decade have revealed phenomena of the electrical double layer that are not captured by either the GC or other theories. For high surface charge densities or high electrolyte concentrations, the ion density profiles in the PM predict a highly organized layering of ions at the charged surface than either the GC or GCS. In particular, for 1:1 electrolytes, the conterion profile shows three distinct layers. For both 1:1 and 2:2 electrolytes at high concentrations, there is charge inversion with coion densities exceeding the counterion density in the second layer. Neither of these phenomena are predicted by the GCS model, although the probable occurrence of both were discussed by Grahame [20] in the interpretation of the interfacial tension measurements of Hg. The obvious disadvantage of the PM is that the interfacial structure of the solvent is minimized, although it is well known that ion solvation and dipole orientation at the surface, both of which are critical in determining the potential and ion distributions, are correlated with the molecular structure of the solvent. The development of realistic models of water and the *civilized* primitive model [21], in which the solvent is treated as a dipole embedded in a hard sphere, allows the effects of the solvent structure on the double layer structure to be studied. The complexity of realistic models of water limits studies of these systems to computational simulations; however, very recent investigations of an electrified Pt/H_2O interface [22] (no ions present) demonstrates the importance of molecular solvent structure on the interface potential distribution.

A recent theoretical study of the civilized primitive model of the electrical double layer by Russier et al. [23] notes the importance of steric effects imposed by the solvent on the ion densities expected at a hard wall. These authors showed that the closest approach of an ion to a neutral wall is determined by electrostatic ion dipole interactions between ion and solvent which is proportional to the inverse square of the distance between the interacting hard spheres and the solvent diameter. The results of Russier et al. are quantitatively different from any previous results found in the PM, in that the closest approach of the ion does not neccesarily correspond to intimate contact between the wall and ion.

In this work, we present Monte Carlo simulations of a *solvent* primitive model (SPM) of the electrical double layer in which the effects due to the finite size of solvent molecules are included. Ion density and potential profiles are compared for electrolytes in contact with charged and neutral walls for several surface charge densities and electrolyte concentrations. The key findings of our present work is that the finite size of the solvent results in highly ordered layering of ions at both charged and neutral walls. For electrolytes comprised of different size anions and cations, the solvent induced structure results in a space charged layer about two molecules thick at a neutral wall.

II. Model System

The systems simulated in this work are mixtures of 1:1 primitive electrolytes and hard sphere solvent molecules contained between two infinite planar surfaces. One of the surfaces (at $z = 0$) is uniformly charged and the other (at $z = H$) is neutral. The charged side of the system is shown schematically in Figure 1 for solvent molecules and ions of diameter d. In the computations, the systems are represented as a periodic array of closed rectangular boxes of height H and a square base of length L on a side. The surface charges on the wall at $z = 0$ is balanced by the excess counterions in the solution. N_+ and N_- and q_+ and q_- are the number and charge of cations and anions in the enclosed system. Electroneutrality requires

$$|N_- q_- - N_+ q_+| = \sigma A \ , \tag{1}$$

where σ is the surface charge density and $A = L^2$. The interaction potential between particles i and j is

$$U(r_{ij}) = \begin{cases} \infty \ , & r_{ij} < (d_i + d_j)/2 \\ \frac{q_i q_j}{\epsilon |r_i - r_j|} \ , & r_{ij} > (d_i + d_j)/2 \ , \end{cases} \tag{2a}$$

and between particle i and the wall is,

$$U(r_i) = \begin{cases} \infty, & z_i < d_i/2 \\ -2\pi\sigma q_i z_i/\epsilon, & z_i > d_i/2 \end{cases}, \tag{2b}$$

where z_i is the distance between the wall and particle i. In equations (2a,b), d_i is the diameter of particle i , q_i equals the ion valence times the unit electronic charge e. ϵ is the dielectric constant (taken to be 78.5 , the value of bulk liquid water, in the simulation). Of course, if either i or j is a neutral particle the Coulomb potential in (2a) or (2b) is zero.

In the simulations the system is periodically extended in the x and y directions. The resulting long range Coulomb potential between ions and their periodic replicas is given by the sum obtained by [7,24]

$$U(r_{ij}) = 4\sum_{l=1}^{\infty}\cos(l\xi)\sum_{-\infty}^{\infty}K_0(l\sqrt{(\eta+2\pi m)^2+\zeta^2}) - \ln(\cosh\zeta - \cos\eta). \tag{3}$$

with the notation that $\xi = 2\pi(x_i - x_j)/L$, $\eta = 2\pi(y_i - y_j)/L$, and $\zeta = 2\pi(z_i - z_j)/L$. $K_0(x)$ is the modified Bessel function which decreases to zero very quickly as x increases.

III. Simulation

In order to run the simulation corresponding to fixed bulk salt concentrations, we first run the grand canonical Monte Carlo (GCMC) simulations for the primitive electrolyte systems in the following way [4-5]. The addition and deletion are attempted with equal probability of about 10 percent and the moves are attempted at 80 percent probability. At each addition or deletion a neutral pair of cations and anions are added or deleted. If the probability of accepting a trial step from state i to state j is f_{ij}, then

$$\frac{f_{ij}}{f_{ji}} = \frac{N_i^+!N_i^-!}{N_j^+!N_j^-!}\exp[B - \beta(U_j - U_i)], \tag{4}$$

where $N_i^{\pm}$ and $N_j^{\pm}$ are the number of cations and anions in states i and j and

$$B = 2\ln\gamma_{\pm} + \ln(n_+V_+) + \ln(n_-V_-)\ , \tag{5}$$

with $\gamma_{\pm}$ the mean ionic activity and n_i is the number density of particle i with $n_i = N_i/V_i$. V_i is the volume accessible to particle i. The Markov chain is set up according to

$$f_{ij} = min(1,\ f_{ij}/f_{ji}) \quad addition,$$

$$f_{ji} = min(1,\ f_{ji}/f_{ij}) \quad deletion, \tag{6}$$

$$f_{ij} = min[1,\ \exp(-\beta U_{ij})] \quad move,$$

where $\beta = 1/kT$ with k is the Boltzmann constant and T is the temperature. In the simulations, T is fixed at 300 Kelvin. The ionic activity coefficients $\ln\gamma_{\pm} = -0.127$ and 0.271 [5] are used in the GCMC simulations respectively for systems $(a-c)$ listed in Table I. For systems d and e, there are no previously available data for $\ln\gamma_{\pm}$. Using equation (4), for a 1 molar 1:1 electrolyte, we obtained the ionic activities from bulk electrolyte GCMC simulations to be $\ln\gamma_{\pm} = -0.318$ and -0.44 for systems d and e, respectively.

For the confined systems, the average number of cations and anions corresponding to the right bulk concentrations of the systems are obtained from GCMC simulations. Subsequently, simulations of the SPM model of the double layer were carried out in the canonical Monte Carlo (CMC) [7] simulations using systems $(a-e)$. The total number of solvent molecules and ions was fixed at

$$(N_+ + N_- + N_0)d^3/HL^2 \sim 0.7, \tag{7}$$

where N_+ and N_- are the average number of free ions in the confined PM fluid. This total number density corresponds roughly to an aqueous solution at 300K. At such high density a grand canonical Monte Carlo simulation is very hard to carry out due to the difficulties in inserting particles. The simulation process can be divided into four steps :

(1) GCMC for bulk $\Rightarrow \ln\gamma_{\pm}$ and bulk concentration C
(2) GCMC for confined system with $\ln\gamma_{\pm}$ and C $\Rightarrow$ Average $N_+ + N_-$
(3) Add solvent $\Rightarrow$ SPM, $nd^3 \sim 0.7$
(4) CMC for SPM

When the electrolyte concentration is 1 molar, the box has a height of $H = 12d$ and base of $L = 4.4d$; reduced surface charge densities of $\sigma^* = \sigma d^2/e = 0.42$ and 0.7, with $d = 4.25$ Å, were used in the simulations. For an electrolyte concentration of 2 molar, $H = 14.14d$ and $L = 4.5d$, and $\sigma^* = 0.40$. These parameters as well as the solvent and ion diameters are listed in Table I. The long range Coulomb interaction is handled by the summation technique given in section II. The probability of acceptance used in the SPM simulations is 10 percent. During the run, the systems were equilibrated for 10^5 steps and then was run $(2.5-4.0)\times 10^6$ to accumulate averages to calculate the density profiles $n(z)$

and the mean electrostatic potential $\psi(z)$. The density $n(z)$ was obtained by counting the number of particles in slices parallel to the walls and dividing by the volume. Very long runs are required compared to the primitive electrolytes simulations, in order to eliminate the noise in the density profiles. $\psi(z)$ is obtained *via* the relation

$$\psi(z) = \frac{4\pi}{\epsilon} \sum_j \int_z^H dz_1 \, (z - z_1) q_j n_j(z_1). \tag{8}$$

Here we take the right wall as the reference point of the potential.

IV. Results and Discussion

In the following we report our simulation results of the density profiles and mean electrostatic potentials for the different systems that are listed in table I. For all the systems studied, the left side wall is charged and the right wall (at $z = H$) is neutral. The surface charge density, the ion and solvent density, and the mean electrostatic potential are reported in the dimensionless forms

$$\sigma^* = \frac{\sigma d^2}{e}, \quad n_i^* = \frac{n_i}{n_{i0}}, \quad and \quad \psi^* = \beta e \psi, \tag{9}$$

where n_{io} is the bulk number density for species i ion and is the number density for tne neutral solvent.

To compare the results obtained here with those obtained for the primitive electrolytes, in figure 2, we show the SPM results as continuous, dotted or dashed curves and the PM results as open and filled circles for the case of $\sigma^* = 0.42$ and $C = 1M$. These PM results were obtained in step (2) of the simulations and agree with previous simulations [4,7]. As is well known, the Gouy-Chapman theory and simulations of the primitive electrolytes are in agreement for low surface charge density and concentration. Both the density profile and the mean electrostatic potential are monotonic. From the figure we can see that, the solvent structure included in the SPM simulation has a dramatic effect on the electrolyte ion profiles. The presence of solvent molecules at the walls induces strong structure in the ion distributions at both charged and neutral walls. Near the left wall, the neutral particles and counterions have five layers, the coions show four layers and near the right wall there are four layers for all particles. A small residue of the coions near the left wall is in the SPM model simulation. These structural features are absent in the PM simulations. Figure 3 shows the mean electrostatic potential for the same system as in figure 2, the

potential decreases rapidly near the charged wall and decays to zero. As mentioned in section III, the noise in the density profiles prevents us from getting more accurate results to see a clear trend of the potential.

Figures 4 and 5 are from the simulations with $\sigma^* = 0.7$ and $C = 1M$. The layering of ions is very distinct as seen in figure 2. Because the strong field on the left wall, the coions were completely repelled from the wall in the PM. However, the hard sphere solvent and ion interactions in the SPM again result in a significant ordering of coions near the charged surface. The mean electrostatic potential of the SPM decreases more rapidly near the charged wall than does that of the PM. The deviations of our simulations are shown in errorbars in both figures 4 and 5. This was obtained from five equal length segments of the simulations with different seeds for the random number generator and started with the previous final configuration as the initial configuration of the new run. Notice that the errorbars for the counterions is $0.1d$ ahead in its z coordinates than the coions and solvent particles in figure 4.

In figures 6 and 7, we change the ion concentration to $2M$ and use $\sigma^* \sim 0.4$. Again the layering of ions is very strong and similar to figures 2 and 3. Furthermore, a charge inversion occured in the second and third layer with the coion density exceeding the counterion.

To see intuitively how a dense solvent will induce significant structure in the ion density distributions even though the ions are present at low concentration, let us consider a dense hard sphere mixture confined by a hard wall. Suppose one component is present at high density and the others are present at low concentrations. Suppose also that all hard sphere species have the same diameter. Then the total density distribution $n(z)$ ($n = \sum_\alpha n_\alpha$) near the wall would be that of a one component hard sphere fluid. At high densities this is known to be a highly oscillatory function. The probability density that any hard sphere will be found at position z is $n(z)/N$ ($N = \sum_\alpha N_\alpha$) and, since the hard spheres all have the same diameter, the probability that this hard sphere is species α is x_α, where x_α is the mole fraction of α. Thus, the probable density $n_\alpha(z)$ of species α at z is $n_\alpha(z) = Nx_\alpha(n(z)/N) = x_\alpha n(z)$. This result shows that the density profiles of all hard sphere species have the same structure, the difference being simply that their ratios $n_\alpha(z)/n_\beta(z)$ scale as their mole fraction ratio x_α/x_β. As indicated by the results shown in Figures 3-7, adding charge to the confined walls and to the electrolyte modulates the density oscillations somewhat, but does not appreciably shift the positions of the maxima and minima from those induced by the hard sphere repulsions.

To examine the effects of ion diameters on the highly structured ion distributions of the SPM, we ran simulations for two different electrolytes comprised of dissimilar sized particles, namely, $d_+ = 0.75d_-$ and $d_+ = 0.5d_-$. The results are given in figures 8 through 11. These results show that the coion peaks shift due to the size effect but there is still significant layering structure in the ion and solvent density distributions. Ion-size induced charge separations is clearly seen near the neutral wall. Due to the noise in the density profiles, we cannot make an accurate estimate of the potentials resulting from these separations. Comparing the density profiles in figures 8 and 10, one can see that the layering seems mainly determined by the larger solvent and counterions near the two walls, even though the effect of the coion size made the peak shift a little. Again these structures are absent in PM electrolytes.

From the above analysis and comparision with the primitive electrolyte simulations we see the essential role of the solvent in determining the structure of electrolytes at solid surfaces. In fact, the layering structures appearing in the SPM electrolytes are mainly due to the high total fluid density resulting from the presence of the solvent molecules. The small residue of coions near the charged surfaces is due to the layering of the solvent and counterions. The fact that we did not observe stronger structures near the charged wall at higher surface charge density ($\sigma^* = 0.7$) than at lower surface charge densities ($\sigma^* \sim 0.4$) confirms the idea that the effect of the solvent plays a more important role in determining the electrolyte structure than solely by the surface charge hard sphere ion interactions, as is the case of the primitive electrolyte. In all cases that have been studied in this paper, the mean electrostatic potential of the SPM is smaller than that obtained from the PM near the charged wall.

Finally, we test our results for consistency by comparing in Table II the simulated difference, $\psi(0) - \psi(d/2)$, with the value of $2\pi\sigma d/\epsilon$, since theoretically

$$\psi(0) = \psi(d/2) + \frac{2\pi\sigma d}{\epsilon} . \tag{10}$$

The numbers in Table II show that the agreement is very good. Also shown in Table II are values obtained by Valleau and coworkers in a grand canonical ensemble simulation of the primitive model electrolyte at the same conditions that we used. Their results also obey eq.(10) quite accurately. Our values of $\psi(0)$ and $\psi(d/2)$ differ somewhat from theirs. The difference perhaps arises from size difference of the simulated systems (they use much larger systems than ours).

The input surface charge density σ agreed with that computed from the ion density distributions,

$$\sigma = \frac{1}{A} \int_{d/2}^{H} \sum_i q_i n_i(z)\, dz, \tag{11}$$

to the fourth digit. This is guaranteed in our simulations by the charge balance of eq.(1).

The apparent structure of the interfaces obtained from the solvent primitive model may provide new insight into the interaction of charged particles near surfaces. The layering of molecules near a surface would be reflected by oscillatory interaction forces. Force measurements using mica surfaces have revealed short range oscillatory electrical double layer forces [25-29].

Acknowledgements

The Minnesota Supercomputer Institute (MSI), the National Science Foundation , and the Office of Naval Research provided support for this work.

References

1. G. Gouy, *J. Phys.* **9**, 457 (1910).
2. D. L. Chapman, *Philos. Mag.* **25**, 508 (1913).
3. O. Stern, *Z. Elektrochem* **30**, 508 (1924).
4. J. P. Valleau, L. K. Cohen, *J. Chem. Phys.* **72**, 5935 (1980). J. P. Valleau, L. K. Cohen, and D. N. Card, *J. Chem Phys.* **72** ,5942 (1980).
5. G. M. Torrie, and J. P. Valleau, *J. Chem. Phys.* **73**, 5807 (1980). S. L. Carnie and G. M. Torrie, *Adv. Chem. Phys.* **56**, 141 (1984).
6. W. J. Van Megen, I. K. Snook, *J. Chem. Phys.* **73**, 4656 (1980), **75**, 4104 (1981).
7. Lianrui Zhang, Henry S. White and H. Ted. Davis, *Proceedings of the 102nd Electrochemical Society Meeting*, Toronto, Canada, 1992; *Molecular Simulations* in press.
8. D. M. Heyes, *Chem. Phys.* **69**,155 (1982).
9. L. Guldbrand, B. Jonsson, H. Wennerstrom, and P. Linse, *J. Chem. Phys.* **80**, 2221 (1984); B. Svenson and B. Josson, *Chem. Phys. Lett.* **108**, 580 (1984). *J. Chem. Phys.* **80**, 2221 (1984).
10. S. H. Suh, L. Mier-y-Teran, H. S. White, and H. T. Davis, *Chem. Phys.* **142**, 203 (1990).
11. D. Levesque, J. J. Weis, and J. P. Hansen, in *Topics in Current Physics* Vol. **36**, Applications of the Monte Carlo Method in Statistical Physics, ed K. Binder (Springer, Berlin, 1984).
12. S. Levine and G. M. Bell, *Discuss. Farad. Soc.* **42**, 69(1966); C. W. Outhwaite and L. B. Bhuiyan, *J. Chem, Phys.* **85**, 4206(1986); and references cited therein.
13. L. Blum,*Adv. Chem. Phys.* **78**,171 (1990); and references cited therein.
14. L. Mier-y-Teran, S. H. Suh, H. S. White, and H. T. Davis, *J. Chem. Phys.* **92**, 5087 (1990); L. Mier-y-Teran, E. Diaz-Herrera, M. Lozada-Cassou, and D. Henderson, *J. Phys. Chem.* **92**,6408(1988); E. J. Boyle, L. E. Scriven and H. T. Davis, *J. Chem. Phys.* **86**, 2309 (1987).
15. R. Evans and T. Sluckn, *Mol. Phys.* 40,413(1984).
16. D. Henderson, F. F. Abraham, and J. A. Barker, *Mol. Phys.* **31**,1291 (1976).
17. M. Born and H. S. Green, *Proc. Roy. Soc. London* **1988**, 10(1946); J. Yvon, *La Theorie Statistique Des Fluides, Paris* (1935).
18. J. G. Kirkwood and E. Monroe, *J. Chem. Phys.* **9**, 514 (1941).

19. R. lovett, C. Y. Mou, and F. P. Buff, *J. Chem. Phys.* **65**, 2377 (1976); M. S. Weitheim, *J. Chem. Phys.* **65**, 2377 (1976).
20. D. C. Grahame, *Chem. Rev.* **41**, 441 (1947).
21. G. N. Pay, G. M. Torrie, and J. P. Valleau, *J. Chem. Phys.* **71**,96(1979); J. Eggebrecht and P. Ozler, *J. Chem. Phys.* **93**, 2004(1990). A. A. Gardner and J. P. Valleau , *J. Chem. Phys.* **86**,4163 (1987). D. Levesque and J. J. Weis *J. Stat. Phys.* 40, 39 (1985).
22. D. A. Rose and I. Benjamin, *J. Chem. Phys.* **95**, 6856(1991).
23. J. P. Badiali, M. Rosinberg, and V. Russier, *Mol. Phys.* **56**,105(1985); M. L. Rosinberg, V. Russier, Badiali, and M. E. Boudh'hir, *Ber. Bunsenges. Phys. Chem.* **91**, 276 (1987); V. Russier, J. P. Badiali, and M. Rosinberg, *J. Electroanal. Chem.*, 220, 213 (1987).
24. J. Lekner, *Physica* **176**, 485 (1991).
25. R. Kjellander and S. Marcelja, *Chem. Phys. Lett.* **142**, 485 (1986).
26. G. Karlstrom, *Chem. Scripta* **25**, 89 (1985).
27. J. N. Israelachvili and G. E. Adams, *J. Chem. Soc. Faraday I* **74**, 975 (1984); J. N. Israelachvili, *Chem. Scripta* **25**, 7 (1985).
28. R. M. Parshley, *J. Colloid Interface Sci.* **80**, 153 (1981); **83**, 531 (1981).
29. D. M. Leneveu, R. P. Rand, and V. A. Parsegian, *Nature* **259**, 601(1975); V. A. Parsegian, N. F. Fuller, and R. P. Rand, *Proc. Natl. Acad. Sci. USA* **279**,258 (1979).

Table I. Parameters used in this paper, $\sigma^* = \sigma d^2/e$, side length L, surface separation H. Number of cations, anions, and neutral particles are N_+ , N_-, and N_0, and $N_c = N_+ + N_-$, $\Delta N = N_- - N_+ = \sigma A$, $A = L \times L$. C is the bulk ion concentration for PM electrolytes in molar. The number of steps run in the simulations are given as Nsteps in unit of 10^6 steps in the last column. In all the cases studied in this paper the neutral solvent particle and the anion have diameter of $d_0 = d_- = d = 4.25$ Å. For systems a–b, c, d and e, $\ln \gamma_\pm = -0.127, 0.271, -0.318$ and -0.44, respectively.

sys	H/d	L/d	d_+/d_-	σ^*	N_c	N_0	ΔN	$C(M)$	$Nsteps/10^6$
a	12.0	4.36	1.0	0.42	26	134	8	1.0	4.0
b	12.0	4.47	1.0	0.70	32	136	14	1.0	2.5
c	14.14	4.5	1.0	0.40	54	146	8	2.0	2.6
d	12.0	4.36	0.75	0.42	26	134	8	1.0	2.5
e	12.0	4.36	0.5	0.42	26	134	8	1.0	2.5

Table II. Results of the SPM (computed in canonical ensemble, CMC) and PM (computed in the grand canonical ensemble,GCMC) simulations of the total potential drop across the double layer $\psi_0^* = \psi^*(0)$ and the diffuse layer mean electrostatic potential $\psi^*(d/2)$ as calculated from eq(8) with a bin size $dz = 0.1d$ and compared with eq(11). For systems d and e, we give the diffuse layer potential at $d/2$. The numbers in parenthesis are the numerical uncertainties determined from consequent simulation segments.

	sys	a	b	c	d	e
SPM	$\psi^*(\frac{d}{2})$	1.11	1.75(0.18)	0.45	1.06	1.32
	ψ_0^*	5.52	9.10(0.18)	4.60	5.47	5.73
	$\psi_0^* - \psi^*(\frac{d}{2})$	4.41	7.35	4.15	4.41	4.41
PM	$\psi^*(\frac{d}{2})$	2.78(0.04)	4.60(0.02)	1.75(0.07)	2.82(0.02)	2.89(0.02)
		3.08(0.1)†	5.71(0.14)†	2.29(0.09)†		
	ψ_0^*	7.19(0.13)	11.95(0.04)	5.90(0.07)	7.23(0.02)	7.30(0.02)
		7.52†	13.10†	6.47†		
	$\psi_0^* - \psi^*(\frac{d}{2})$	4.41	7.35	4.15	4.41	4.41
		4.44†	7.39†	4.18†		
	$\frac{2\pi\sigma d}{\epsilon}$	4.41	7.356	4.16	4.41	4.41

† GCMC simulations from reference [5].

Figure Captions

Figure 1. Schematic representation of solvent molecules and ions of diameter d near a uniformly charged flat, impenetrable wall.

Figure 2. Reduced Density profiles $n^*(z) = n(z)/n_0$ for a 1:1 electrolyte at C=1M and $d_+ = d_- = d = 4.25$ Å. The left wall has a surface charge density of $\sigma^* = \sigma d^2/e = 0.42$ and the right wall is uncharged.

Figure 3. Reduce Mean electrostatic potential $\psi^*(z)$ for a 1:1 electrolyte for the same conditions as in figure 1.

Figure 4. Reduced Density profiles $n^*(z)$ for a 1:1 electrolyte at C=1M and $\sigma^* = 0.7$. Other conditions and keys are the same as in figure 1. The errorbars for the counterions are $0.1d$ ahead in the z coordinates than the coions and solvent particles.

Figure 5. Reduce Mean electrostatic potential $\psi^*(z)$ for a 1:1 electrolyte for the same conditions as in figure 3. Errorbars are shown for SPM.

Figure 6. Reduced Density profiles $n^*(z)$ for a 1:1 electrolyte at C=2M and $\sigma^* = 0.40$. Other conditions and keys are the same as in figure 1.

Figure 7. Reduce Mean electrostatic potential $\psi^*(z)$ for a 1:1 electrolyte for the same conditions as in figure 5.

Figure 8. Reduced Density profiles $n^*(z)$ for a 1:1 electrolyte at C=1M and $\sigma^* = 0.42$. $d_+ = \frac{3}{4}d_-$. Other conditions and keys are the same as in figure 1.

Figure 9. Reduce Mean electrostatic potential $\psi^*(z)$ for a 1:1 electrolyte for the same conditions as in figure 9.

Figure 10. Reduced Density profiles $n^*(z)$ for a 1:1 electrolyte at C=1M and $\sigma^* = 0.42$. $d_+ = \frac{1}{2}d_-$. Other conditions and keys are the same as in figure 1.

Figure 11. Reduce Mean electrostatic potential $\psi^*(z)$ for a 1:1 electrolyte for the same conditions as in figure 7.

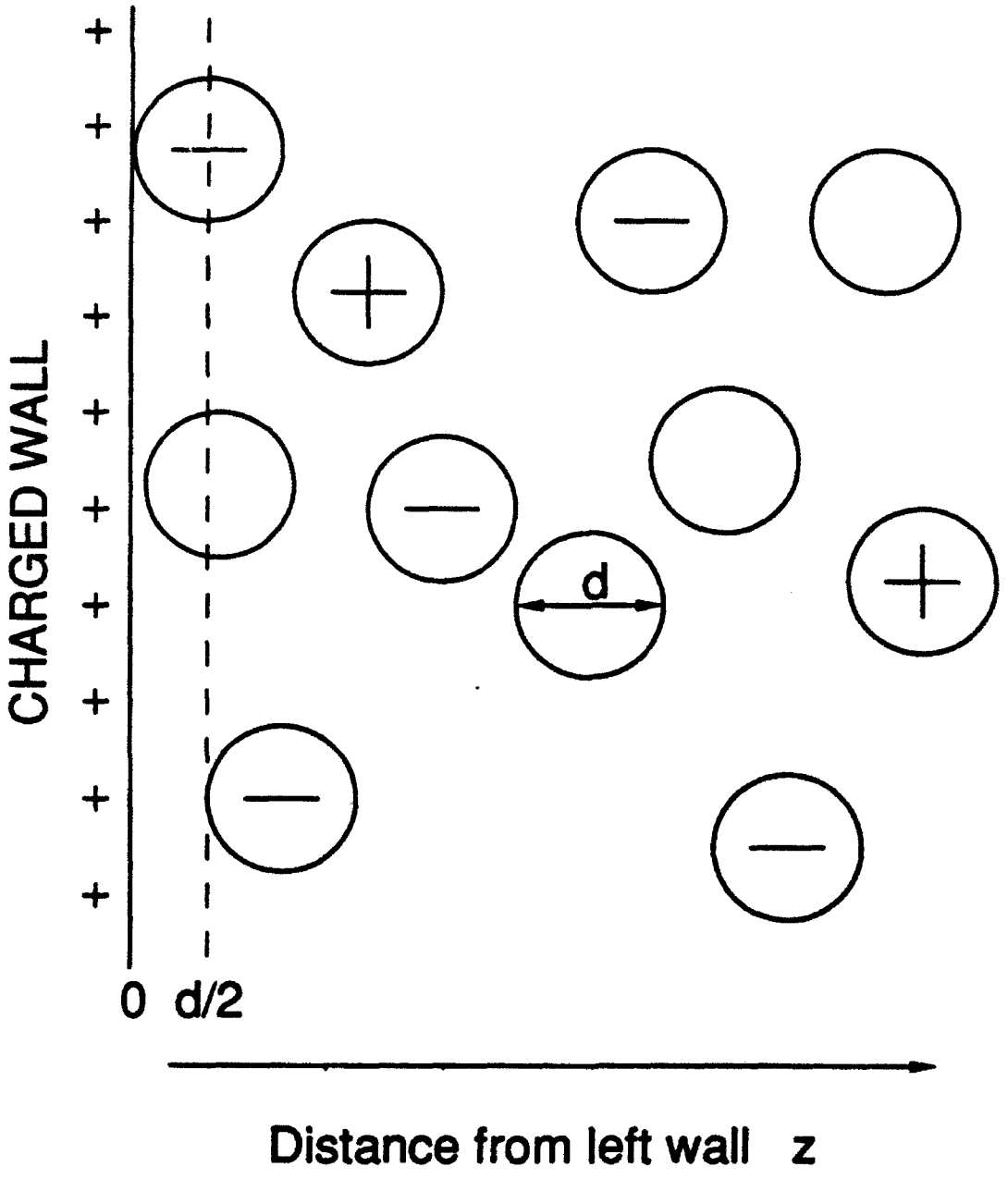

Figure 1

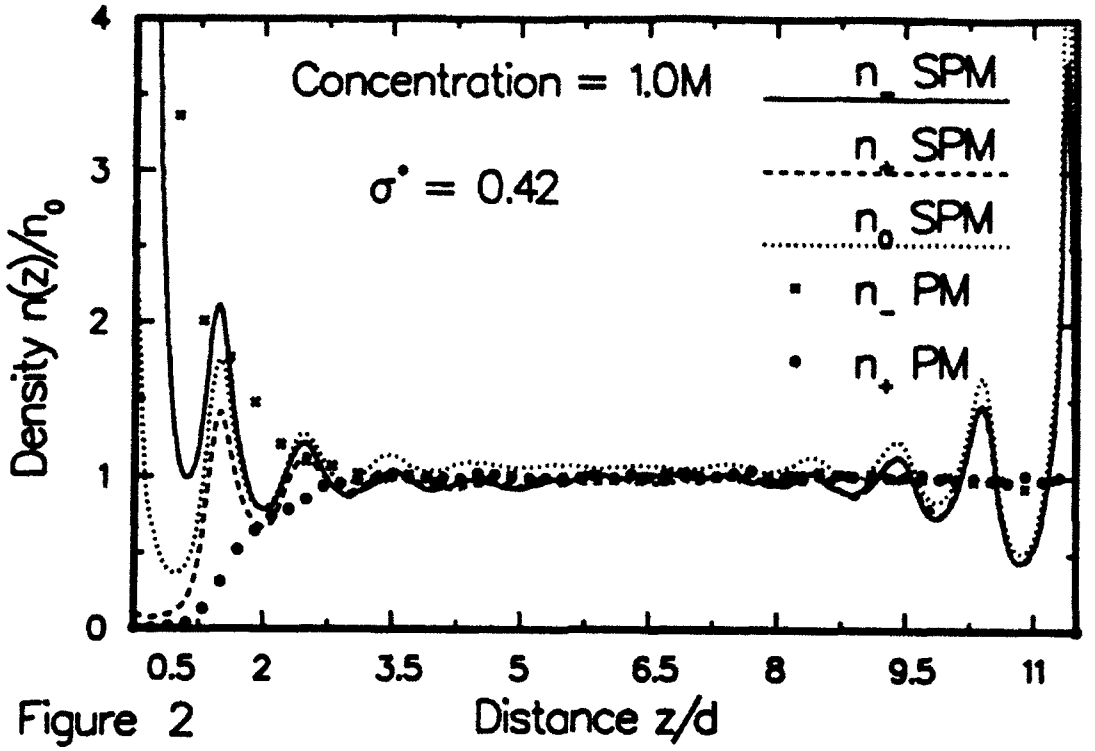

Figure 2

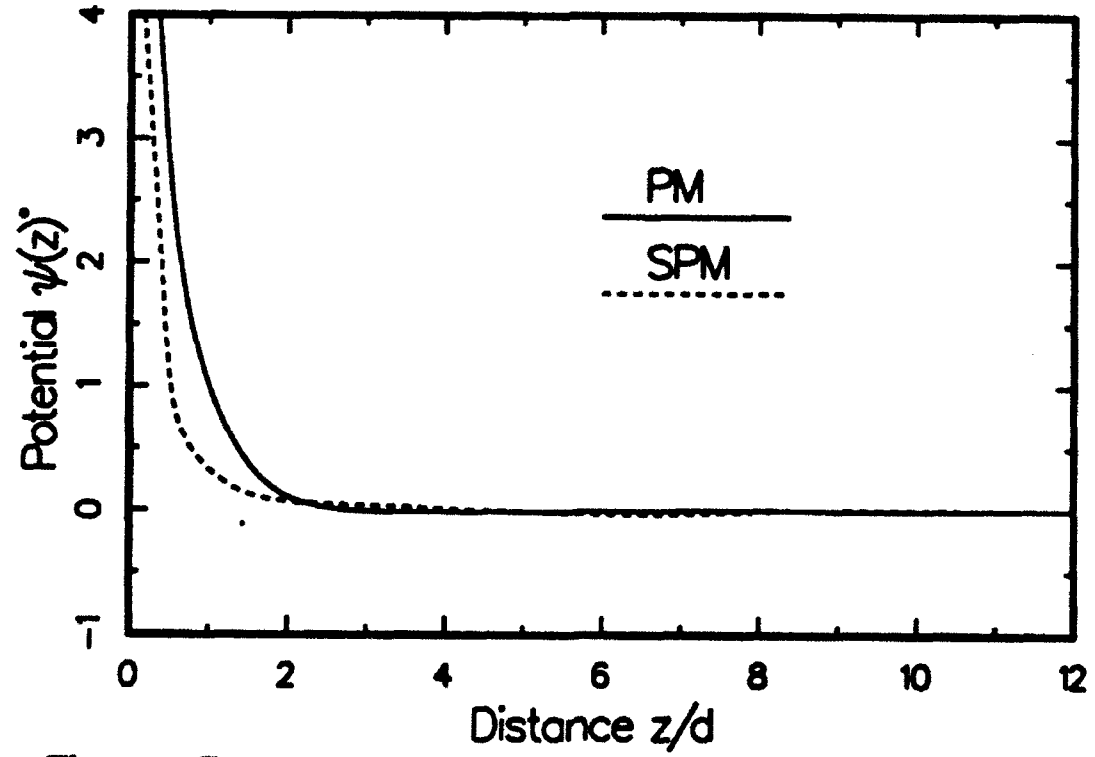

Figure 3

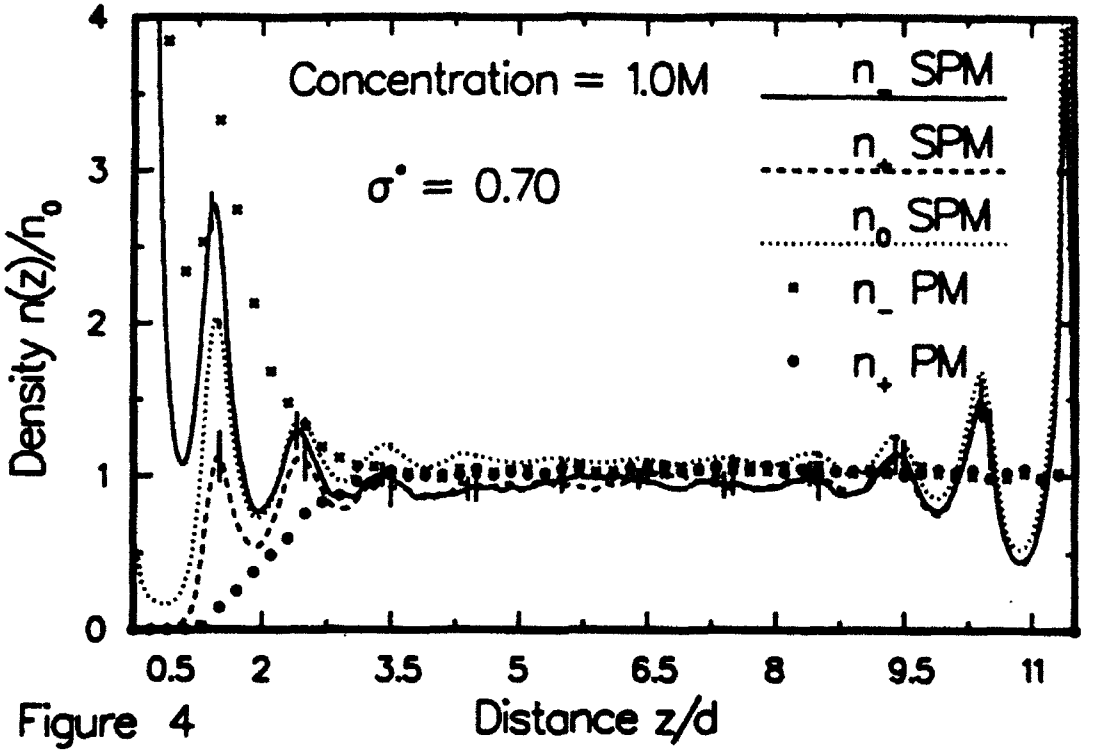

Figure 4

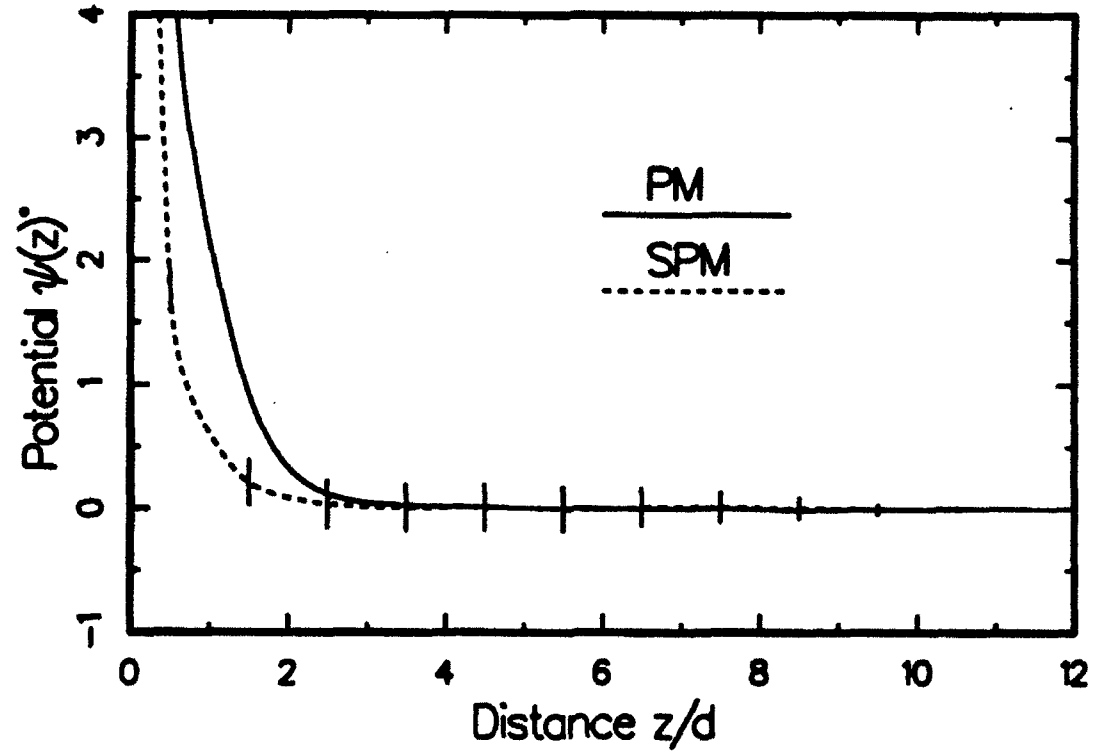

Figure 5

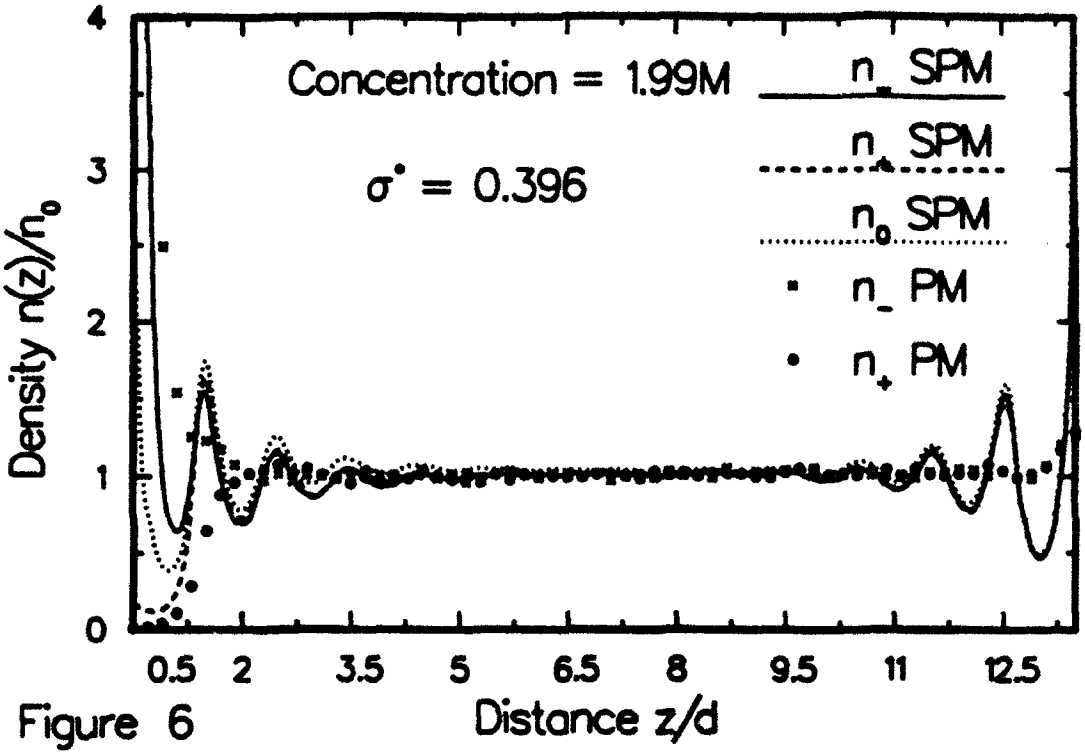

Figure 6

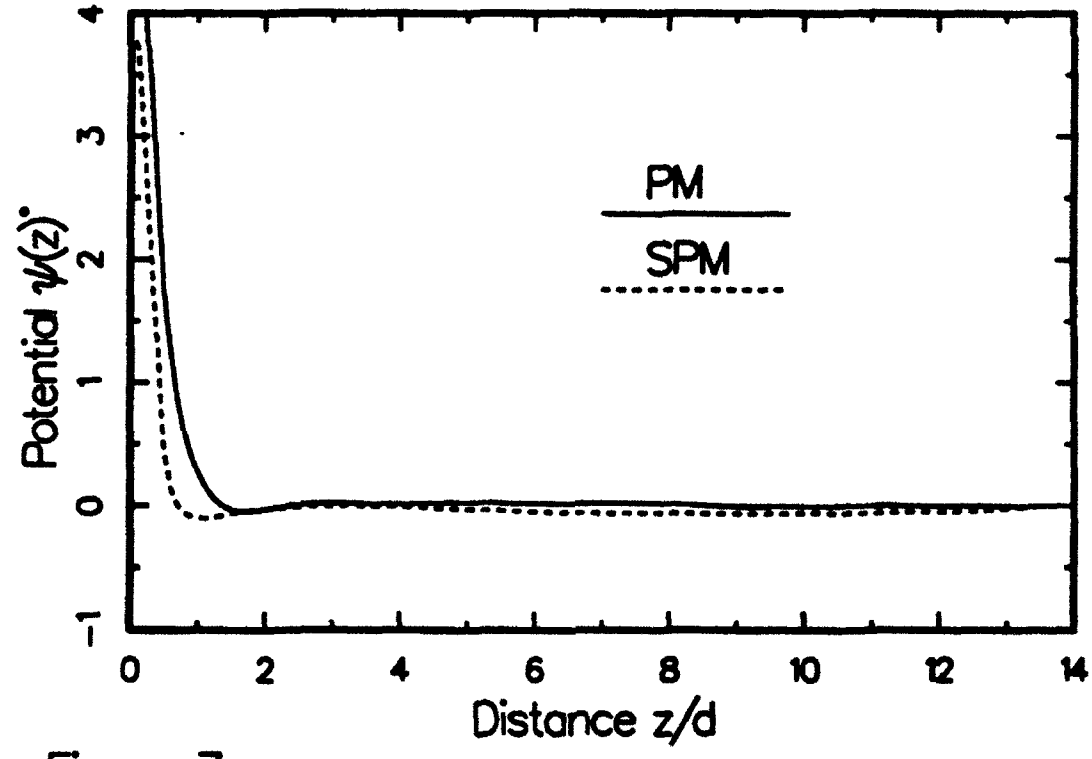

Figure 7

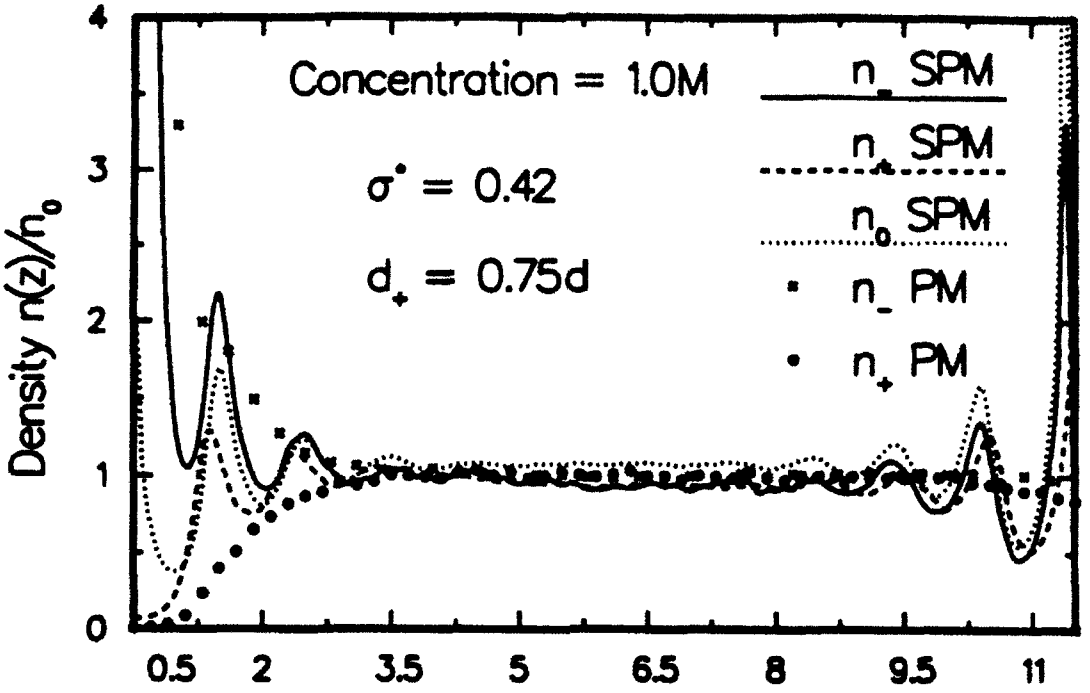

Figure 8

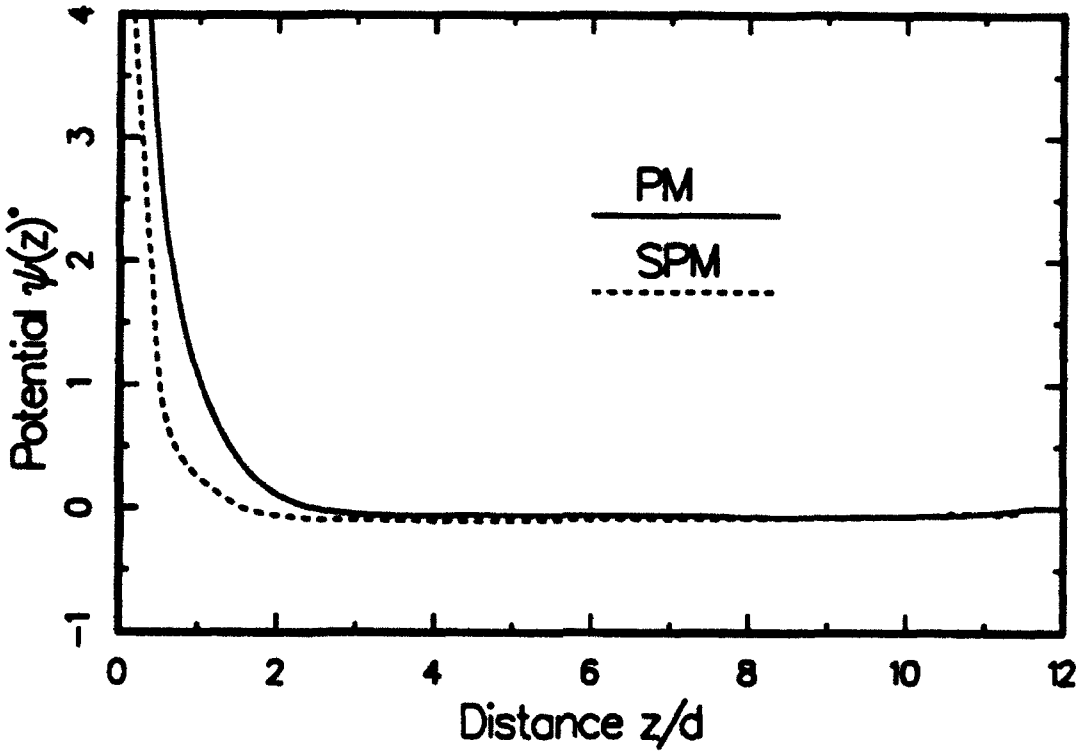

Figure 9

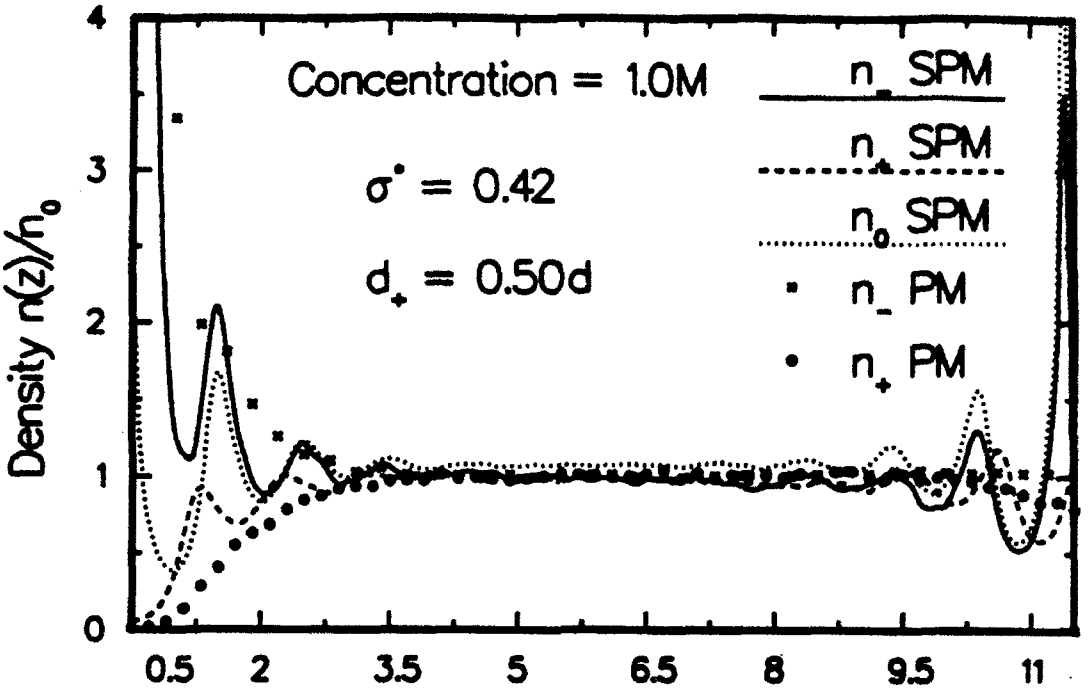

Figure 10

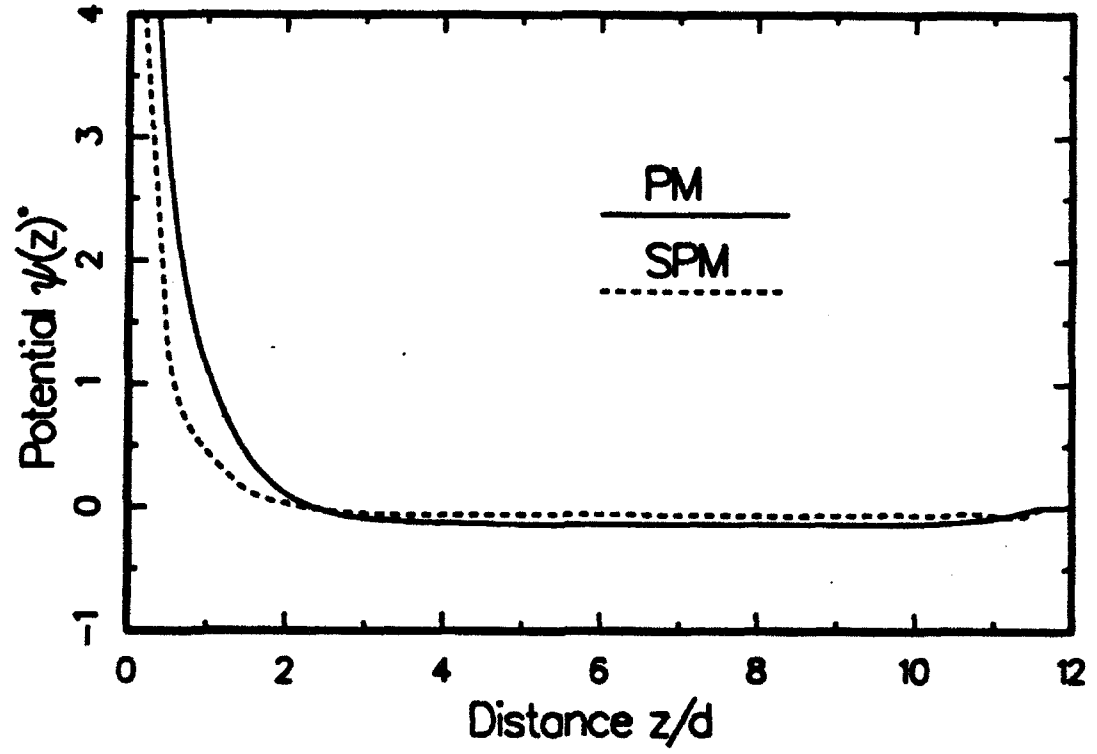

Figure 11